

Supporting Information for:  
**Effect of Sb-Bi alloying on electron-hole recombination time  
of Cs<sub>2</sub>AgBiBr<sub>6</sub> double perovskite**

Yuzhuo Lv<sup>1</sup>, Chang Liu<sup>1</sup>, Yuhang Ma<sup>1</sup>, Guodong Liu, Fei Wang, Yuhong Xia, Chundan Lin,

Changjin Shao

and Zhenqing Yang <sup>†</sup>

Basic Research Center for Energy Interdisciplinary , Beijing Key Laboratory of  
Optical Detection Technology for Oil and Gas, College of Science, China University  
of Petroleum, Beijing 102249, P. R. China

<sup>1</sup> Yuzhuo Lv, Chang Liu and Yuhang Ma contributed equally to this paper.

Yuzhuo Lv : writing-original draft

Chang Liu: writing-review & editing/investigation

Yuhang Ma : conceptualization/methodology/data curation

Guodong Liu: writing/revision/finalization

Chundan Lin : supervision/project administration

Changjin Shao : supervision/project administration

Zhenqing Yang : supervision/project administration

# I Explanation of the Doping Ratio Determination

Hutter and Eline M's research group demonstrated through experiments that among the three proportions of Sb doping (0.05, 0.1, and 0.4), the 0.4 proportion exhibits superior light absorption capabilities.<sup>1</sup> Inspired by these experiments and considering the crystal structure and the number of atoms, we ultimately decided to choose a doping proportion of 0.375, which is closer to 0.4. Additionally, we evaluated four different doping proportions through first-principles calculations, with Sb proportions ranging from smallest to largest: 0.125, 0.25, 0.375, and 0.5. The calculated band gaps are shown in the figure below:

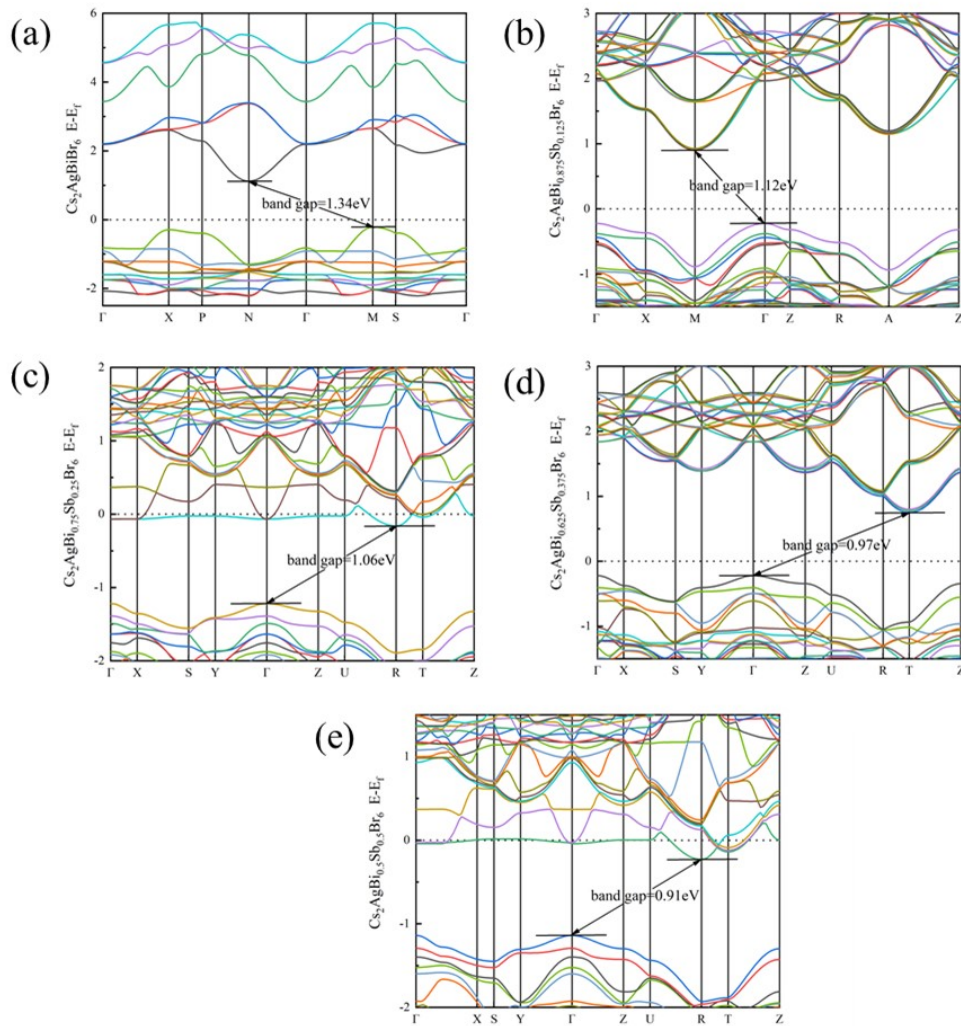


Figure S1. Crystal band diagram of (a) Cs<sub>2</sub>AgBiBr<sub>6</sub> (b) Cs<sub>2</sub>AgBi<sub>0.875</sub>Sb<sub>0.125</sub>Br<sub>6</sub> (c)

Cs<sub>2</sub>AgBi<sub>0.75</sub>Sb<sub>0.25</sub>Br<sub>6</sub> (d) Cs<sub>2</sub>AgBi<sub>0.625</sub>Sb<sub>0.375</sub>Br<sub>6</sub> (e) Cs<sub>2</sub>AgBi<sub>0.5</sub>Sb<sub>0.5</sub>Br<sub>6</sub>.

Due to limited computational resources, we used the PBE functional, which tends to underestimate the band gap to some extent. In contrast, the HSE06 method is closer to the experimental values. Based on experience, the band gap values obtained from HSE06 and PBE have the following relationship:  $HSE06 = 1.21 * PBE + 0.36$ . The band gap values obtained from this formula are shown in the table below:

**Table S1. Bandgap results of PBE method and HSE06 method**

Band	$E_g^{PBE}$ (eV)	$E_g^{HSE06 + SOC}$ (eV)
Cs <sub>2</sub> AgBiBr <sub>6</sub>	1.34	1.98
Cs <sub>2</sub> AgBi <sub>0.875</sub> Sb <sub>0.125</sub> Br <sub>6</sub>	1.12	1.72
Cs <sub>2</sub> AgBi <sub>0.75</sub> Sb <sub>0.25</sub> Br <sub>6</sub>	1.06	1.64
Cs <sub>2</sub> AgBi <sub>0.625</sub> Sb <sub>0.375</sub> Br <sub>6</sub>	0.97	1.53
Cs <sub>2</sub> AgBi <sub>0.5</sub> Sb <sub>0.5</sub> Br <sub>6</sub>	0.91	1.46

Generally, for single-junction solar cells, a band gap between 1.4 eV and 1.6 eV is considered an appropriate range, as it is more conducive to light absorption and exhibits superior photoelectric performance. The band gaps of Cs<sub>2</sub>AgBi<sub>0.625</sub>Sb<sub>0.375</sub>Br<sub>6</sub> and Cs<sub>2</sub>AgBi<sub>0.5</sub>Sb<sub>0.5</sub>Br<sub>6</sub> are 1.53 eV and 1.46 eV, respectively, which fall within the ideal band gap range of 1.4 eV to 1.6 eV for perovskite solar cells.<sup>2</sup>

In addition, we considered photoelectric performance. The Cs<sub>2</sub>AgBi<sub>0.625</sub>Sb<sub>0.375</sub>Br<sub>6</sub> and Cs<sub>2</sub>AgBi<sub>0.5</sub>Sb<sub>0.5</sub>Br<sub>6</sub> systems exhibit stronger light absorption capabilities, and Cs<sub>2</sub>AgBi<sub>0.875</sub>Sb<sub>0.125</sub>Br<sub>6</sub> and Cs<sub>2</sub>AgBi<sub>0.625</sub>Sb<sub>0.375</sub>Br<sub>6</sub> have lower energy losses. Figure S2 and Figure S3 show their visible light absorption spectra and the refractive index,

reflectance, extinction coefficient, and energy loss function within the visible light range, respectively.  $\text{Cs}_2\text{AgBi}_{0.625}\text{Sb}_{0.375}\text{Br}_6$  demonstrates superior performance in terms of band gap and light absorption. We speculate that doping Bi in the original system with Sb at a ratio of 0.375 will be more beneficial for improving the photoelectric conversion efficiency of  $\text{Cs}_2\text{AgBiBr}_6$ .

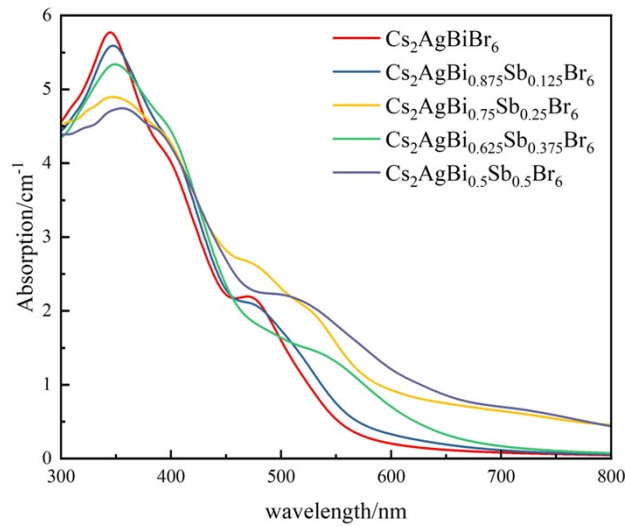


Figure S2. Visible light absorption spectrum of  $\text{Cs}_2\text{AgBiBr}_6$ ,  $\text{Cs}_2\text{AgBi}_{0.875}\text{Sb}_{0.125}\text{Br}_6$ ,  $\text{Cs}_2\text{AgBi}_{0.75}\text{Sb}_{0.25}\text{Br}_6$ ,  $\text{Cs}_2\text{AgBi}_{0.625}\text{Sb}_{0.375}\text{Br}_6$ ,  $\text{Cs}_2\text{AgBi}_{0.5}\text{Sb}_{0.5}\text{Br}_6$ .

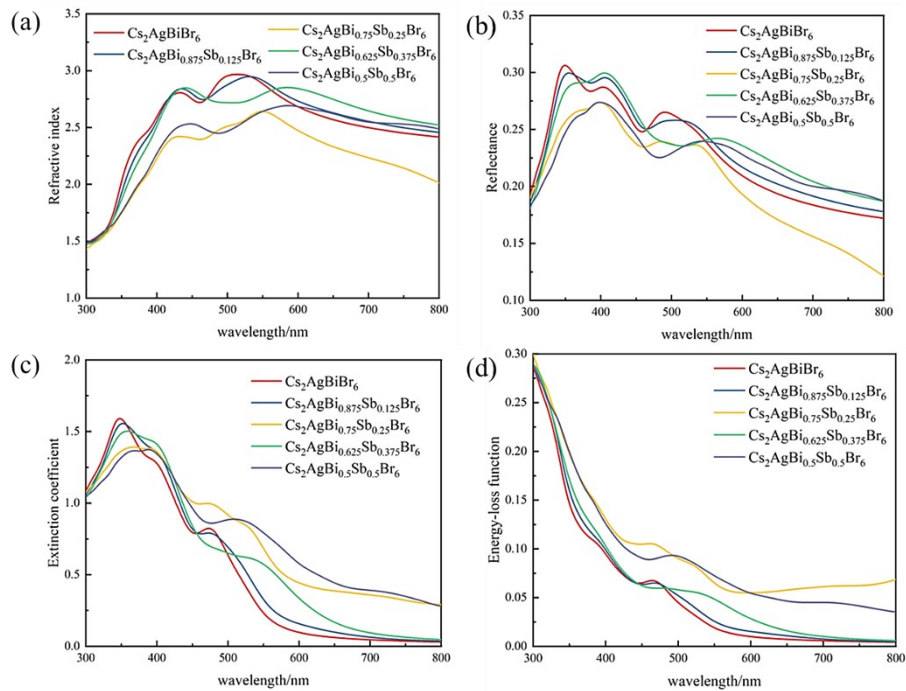


Figure S3. Refractive index (b) Reflectance (c) Extinction coefficient and (d) Energy-loss function for the five systems in the visible light range.

Due to the enormous computational demands associated with accurately sampling a large number of atoms in excited-state dynamics, we ultimately chose to conduct nonadiabatic molecular dynamics calculations on the more promising  $\text{Cs}_2\text{AgBi}_{0.625}\text{Sb}_{0.375}\text{Br}_6$  double perovskite alloy system to explore its photophysical mechanisms.

## II Others

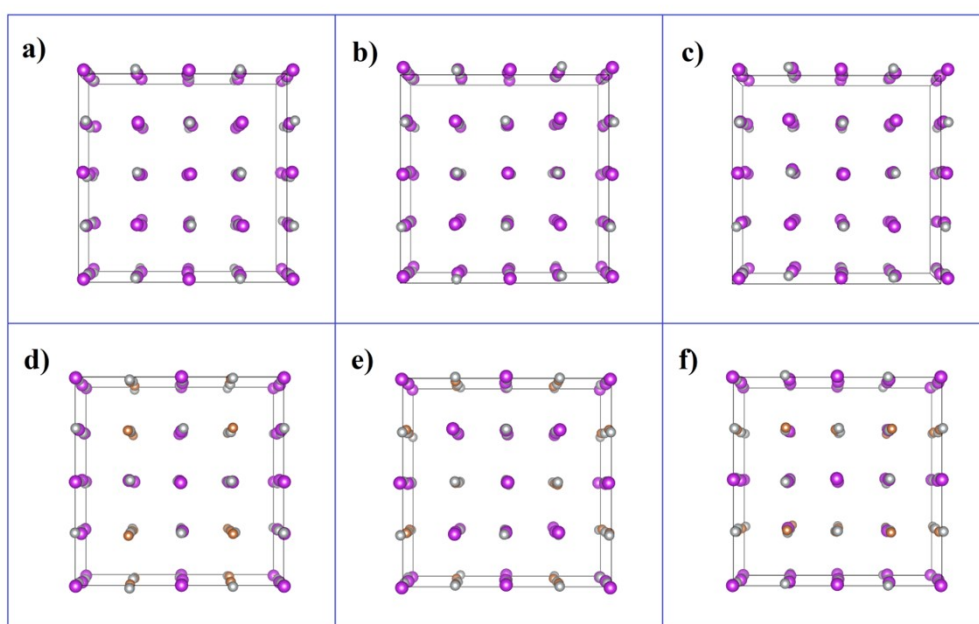


Figure S4. Perspective views of the central skeleton of the octahedron in the unit cell of a) - c)

$\text{Cs}_2\text{AgBiBr}_6$  and d) - f) the doped sample  $\text{Cs}_2\text{AgSb}_{0.375}\text{Bi}_{0.625}\text{Br}_6$ , from left to right are cross-sectional perspectives on the 001, 010, and the 100 crystal plane.

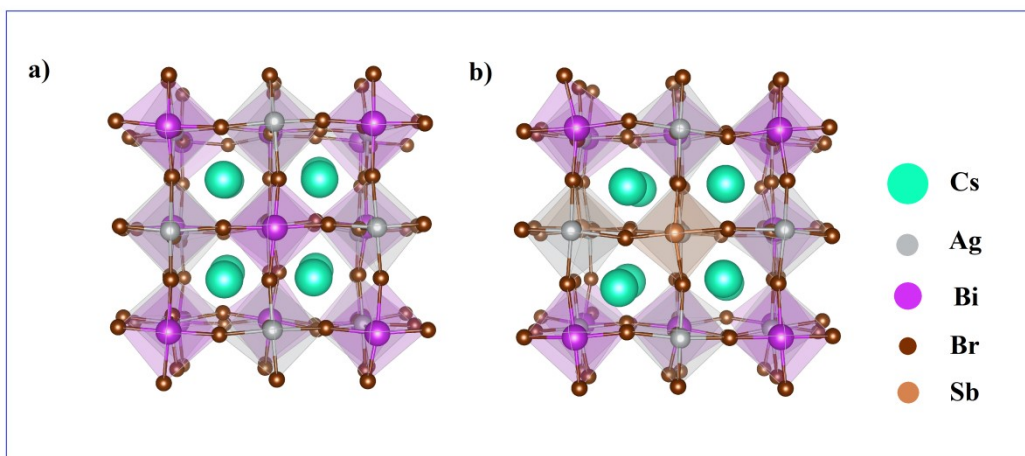


Figure S5. The local octahedral configuration diagram of the unit cells at room temperature for a)

$\text{Cs}_2\text{AgBiBr}_6$ , b)  $\text{Cs}_2\text{AgSb}_{0.375}\text{Bi}_{0.625}\text{Br}_6$ .

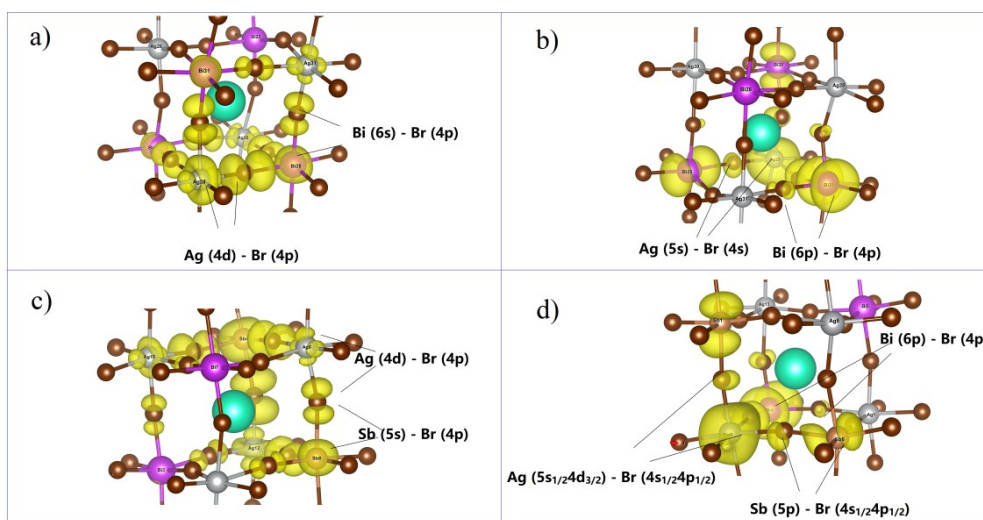


Figure S6. a) and c) are the charge density images of the highest occupied orbital for the pristine sample and the alloyed sample, respectively. b) and d) are the charge density images of the lowest unoccupied orbital for the pristine sample and the alloyed sample, respectively.

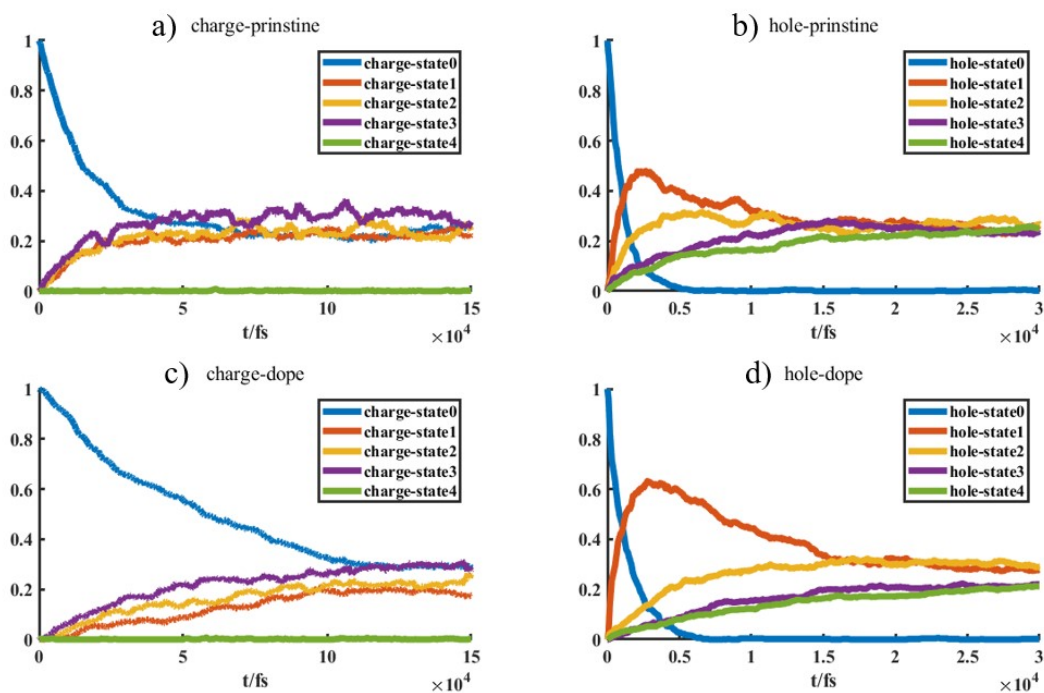


Figure S7. a) and b) Time-dependent orbital population evolution curves for electrons and holes in the pristine sample, while c) and d) are those in the alloyed sample.

## References

- 1 E. M. Hutter, M. C. Gélvez-Rueda, D. Bartesaghi, F. C. Grozema and T. J. Savenije, Band-Like Charge Transport in  $\text{Cs}_2\text{AgBiBr}_6$  and Mixed Antimony–Bismuth  $\text{Cs}_2\text{AgBi}_{1-x}\text{Sb}_x\text{Br}_6$  Halide Double Perovskites, *ACS Omega*, 2018, **3**, 11655–11662.
- 2 C. Lin, Y. Zhao, Y. Liu, W. Zhang, C. Shao and Z. Yang, The bandgap regulation and optical properties of alloyed  $\text{Cs}_2\text{NaSbX}_6$  ( $X=\text{Cl}, \text{Br}, \text{I}$ ) systems with first principle method, *Journal of Materials Research and Technology*, 2021, **11**, 1645–1653.